Effects of concomitancy of adiabatic Betatron deceleration & acceleration (i), of up & down lifting of mirror points altitudes (ii), and of pitch angle scattering (iii) during geomagnetic storms

J.F. Lemaire
K. Borremans
V. Pierrard

Belgian Institute for Space Aeronomy – Brussels

EGU General Assembly 2013, Session ST2.3: EGU2013-13889

Early RB observations and modelling

Based on Explorer XV measurements of 0.5 MeV outer belt electrons, Carl McIlwain listed five general processes to expain the time variations of relatistivistic electrons during geomagnetic storms and in the time between them. (***Mc Ilwain, 1960, 1966, 1996)***

These five processes are sketched in Fig. 1

McIlwain, C.E.*, Processes acting upon outer zone electrons, in « Radiation belts : Models and Standards », pp. 15-26, Geophysical Monograph 97, AGU, 1996*

Fig. 1

18 PROCESSES ACTING UPON OUTER ZONE ELECTRONS

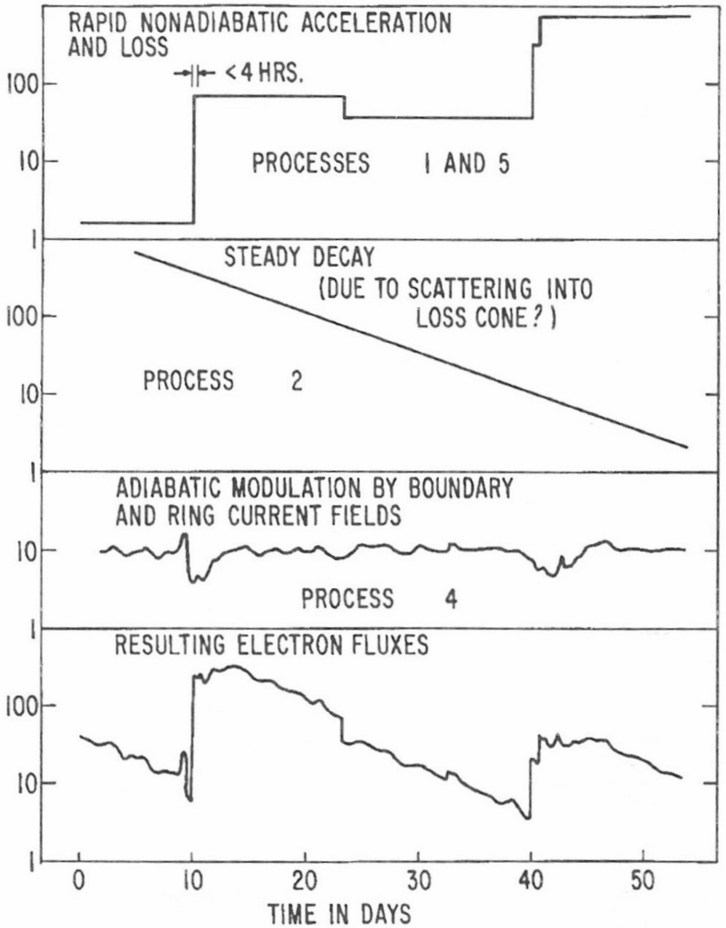

Figure 3. Characteristic effects of Processes 1, 2, 4, and 5 and their combined effect upon the energetic electrons in the outer zone.

***McIlwain, C.E.**, Processes acting upon outer zone electrons, in « Radiation belts : Models and Standards », pp. 15-26, Geophysical Monograph 97, AGU, 1996*

In 1966, McIlwain developed the first detailled mathematical model describing how the flux of RB electrons varies as a function of Dst during small geomagnetic storms of less then - 50 nT. This simple empirical model is founded on the adiabatic Betatron mechanism (process 4 in Fig. 1).

This first empirical model was restricted for relativistic electrons trapped in the outer RB belt near the equatorial plane.

The application of this adiabatic Betatron model, and its validation by using Explorer XV measurements is shown in Fig. 2

***McIlwain, C.E.**, Processes acting upon outer zone electrons, in « Radiation belts : Models and Standards », pp. 15-26, Geophysical Monograph 97, AGU, 1996*

Fig. 2

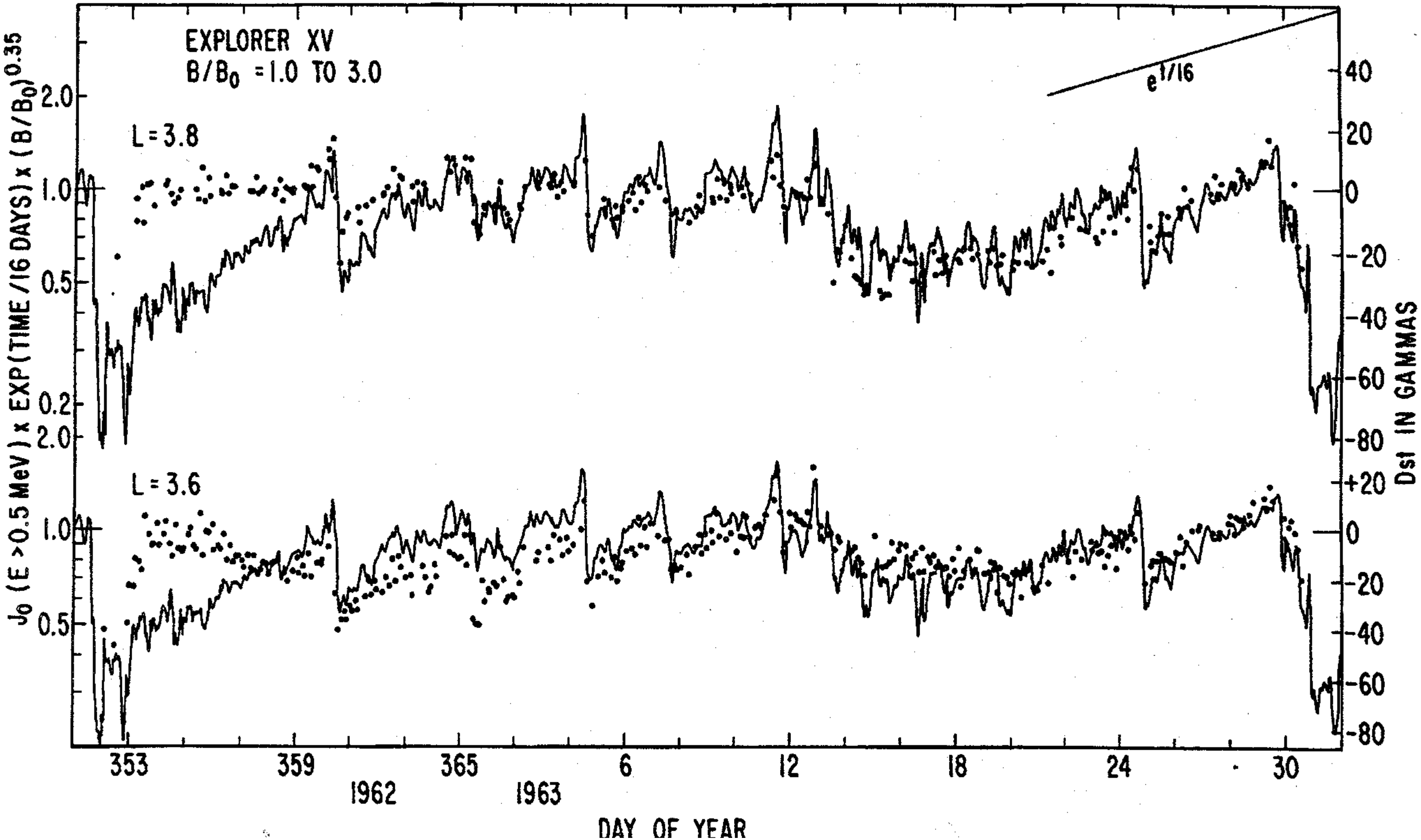
EXPLORER XV
B/B0 = 1.0 TO 3.0
L = 3.8
L = 3.6
e1/16
J0 (E > 0.5 MeV) x EXP(TIME/16 DAYS) x (B/B0)0.35
Dst IN GAMMAS
2.0
1.0
0.5
0.2
40
20
0
-20
-40
-60
-80
+20
353
359
365
6
12
18
24
30
1962
1963
DAY OF YEAR

Adiabatic Radiation Belt flux variations : the « Dst-effect »

Kim and Chan (1997) expanded McIlwain's work : the adiabatic Betatron RB model. It became better known after it had been renamed the 'Dst-effect' model.

This new Betatron RB model did not take into account external sources (injections) nor losses (wave-particle interactions, magnetopause shadowing effects, nor particle precipitation in the atmosphere...).

Under these ideal circumstances the post-storm flux of electrons is necessarily identical to its pre-storm value. This expected because of the adiabaticity of the motion of all trapped particles forming the RB.

It is considered that process N° 4 (adiabatic Betatron or Dst-effect in Fig. 1) is well understood and was comprehensively modelled.

Kim H.J. and Chan A.A., *Fully adiabatic changes in storm time relativistic electron fluxes, Journal of Geophysical Research Vol: 102 , 22107, 1997*

Rapid non-adiabatic acceleration and loss

Beside the « *persistent exponential decay with about a two-week time-constant due to scattering into the loss cone* » (Process N°2 in Fig.1), **McIlwain (1964, 1966)** pointed out the existence of « *rapid non-adiabatic acceleration* » in the EXPLORER XV measurements of 0.5 MeV electrons (Process N°1 and 5 in Fig.1).

Detailed examination indicated that « significant acceleration occurs within only a few hours of time ». But this occurs only during certain geomagnetic storm events. The very reason of this discrimination has been and remains an unsolved issue!

Resonant w-p interactions of relativistic electrons with VLF, ULF or EMIC waves are often invoked to explain these accelerations events and RB flux enhancements.

But if resonant w-p should be able to accelerate relativistic electrons, as is currently believed, a question remains unsolved : how to explain then « rapid losses » i.e. fast reductions of particle fluxes observed from time to time in satellite data.

Possible new solutions

We believe that the concomitant and combined effects of (i) *Betatron acceleration,* (including uplifting of the altitudes of mirror points), and (ii) *non-resonant pitch angle scattering* by waves, contribute to the non-adiabatic process which is needed to accelerate the relativistic electrons and produce the observed « *rapid non-adiabatic flux enhancements » .*

This is the main objective of the present presentation.

Futhermore, we consider that the continual acceleration of trapped RB particles by the « *ponderomotive force* » of magnetospheric Alfvén waves is the additional physical process and source of energization that is unfortunately ignored, despite it had been suggested and modeled in the past by ***Allan (1990, 1991,1993).***

Allan W., *The ponderomotive force of standing Alfvén waves in a dipolar magnetosphere, JGR 98, pp. 1409-1417, 1993*

Trajectories of charged particles in magnetic dipole (B_{dip}) + uniform NBz magnetic field [F(t) : *IMF or Dst*]

When F(t) or Dst decrease as a function of universal time (t)

- an eastward electric field, **E**(t), is induced in space: $-\partial \mathbf{B}/\partial t = \text{curl } \mathbf{E}$
- inside the Ring Current the equatorial magnetic field intensity (B_{eq}) decreases with time,
- drift shells expand and L increases (: conservation of magnetic flux, third invariant).
- the perpendicular kinetic energies ($W_\perp$) of charged particles decrease when t increases (: conservation of first adiabatic invariant : $\mu = W / B_m$)

$$\Delta W = W \, \Delta B_m / B_m \quad \begin{cases} < 0 \text{ when } \Delta B_m < 0 \text{ (in equatorial region : } \Lambda < 32°) \\ > 0 \text{ when } \Delta B_m > 0 \text{ (in midlatitude regions)} \end{cases}$$

*All these effects are consequences of the Betatron mechanism on trapped magnetospheric particles during main phase of geomagnetic storm*s.

Fig. 3

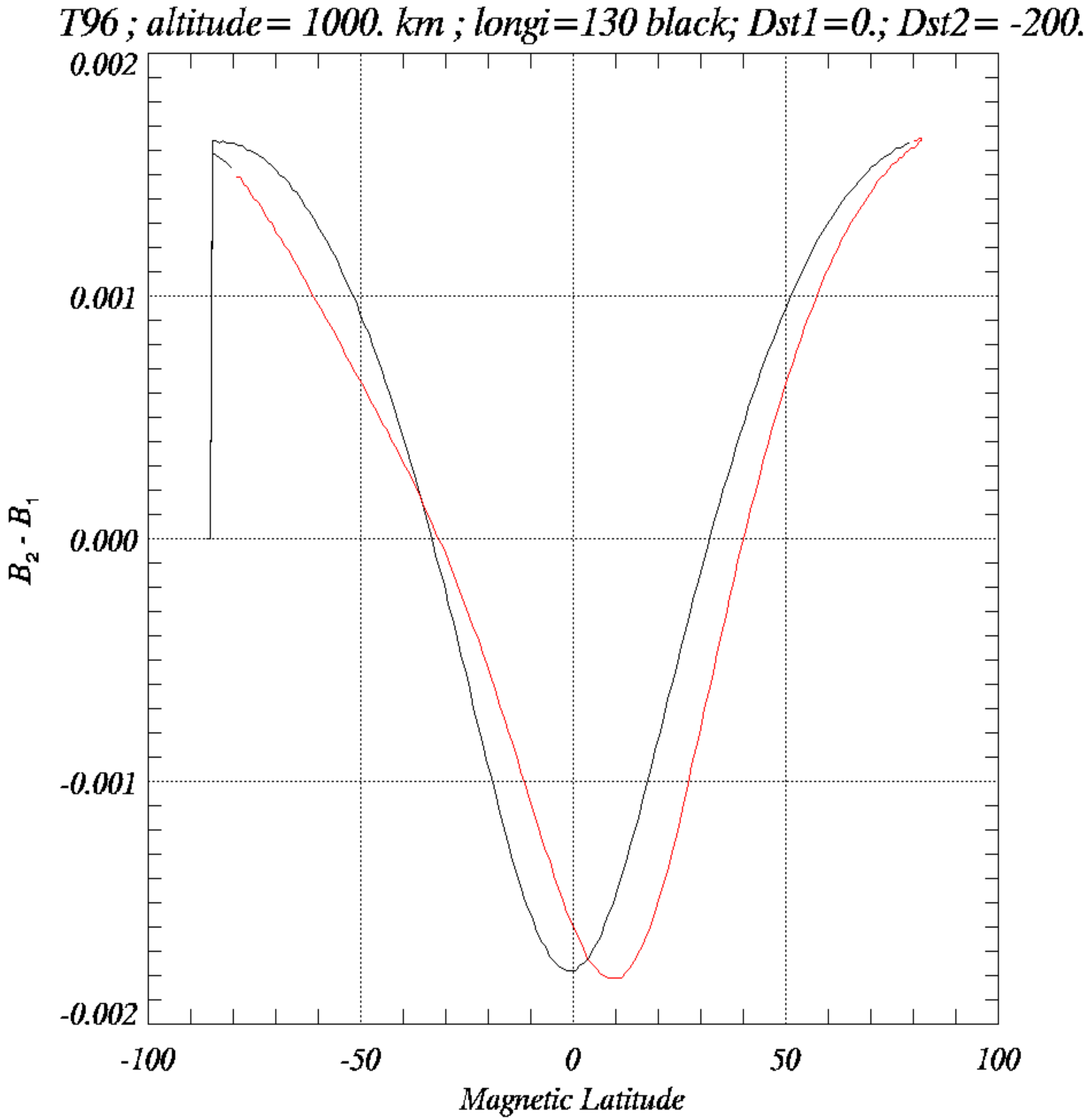

Difference of magnetic field intensities ($\Delta B = B_2 - B_1$) versus latitudes from Tsyganenko's geomagnetic field model (T96) :
B_1 corresponds to Dst = 0 ; while
B_2 corresponds to Dst = -200 nT.

The values of $\Delta B = B_2 - B_1$ are calculated at a constant altitude (1000 km), in two meridional planes. The black curve is for a longitude of 130°E ; while the red curve is for the longitude of the SAA, 230° E).

Note that $\Delta B < 0$ for $-40° < \lambda < +45°$. Since in the equatorial region $\Delta B < 0$ and all particles are decelerated upwards ($\Delta W < 0$) in that region, during main phases :
i.e. when d Dst /dt is negative.
The reverse occurs during recovery phases when d Dst /dt is positive.

On the contrary at midlatitudes for $|\lambda| > 45°$, the reverse situation is obtained : $\Delta W > 0$ since there $\Delta B > 0$ during main phases when d Dst /dt < 0.

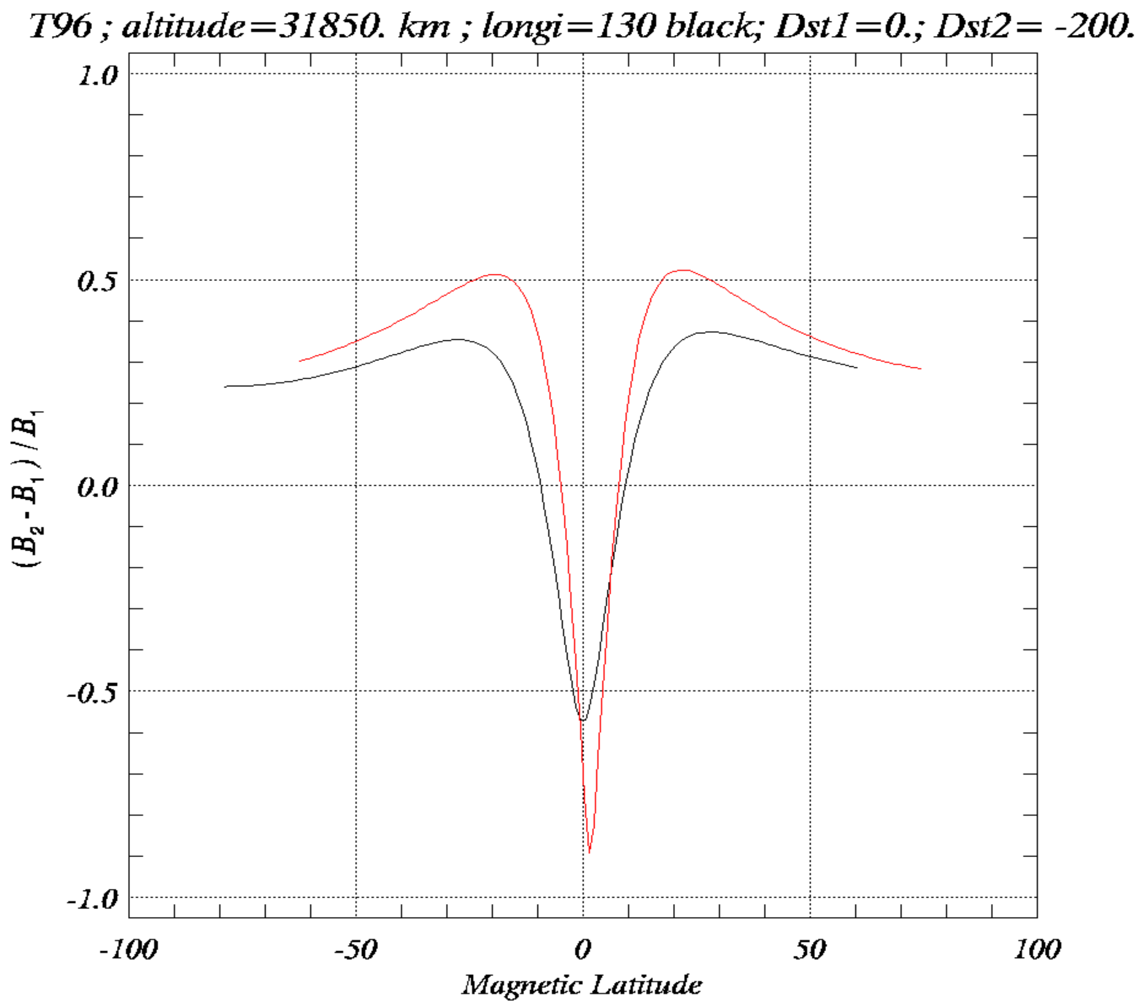

Fig. 4

Same as in Fig. 3 but for a constant altitude of 31830 km.

The relative differences of the B-field intensities (B_1 and B_2) are displayed.

Note that the range of equatorial latitudes where the Betatron mechanism declerates the particles during main phases, is narower at this high altitude, than it is at 1000 km (cnf. Fig. 3).

Altitudes of mirror points

The altitudes of the guiding centers (GC) of particles launched from an equatorial distance ($L\,R_E$), with an equatorial pitch angle of 90°, are moving upwards during main phases of storms, i.e. when Dst or B_{eq} decrease.

The change of GC radial distances and mirror point altitudes (h_m) can be determined by :

$$\Delta h_m(t) \sim -(1/3)\, R_E\, L^3\, \Delta B_{eq} / B_E$$

$B(r) \sim r^{-3}$; $B_E = 31000$ nT ; $\Delta B_{eq} = \Delta Dst < 0$

(an approximation valid near the equatorial pllane)

For $h_m = 2\,R_E$ ($L = 3$) in the equatorial plane the GC of a particle of any energy will move upward by 92 km when Dst changes from Dst = 0 to -50nT : when $\Delta B_{eq} = -50$nT,

$\Delta h_m = -(1/3) * 6371 * 3^3 * (-50\text{ nT}) / 31000\text{ nT} = 92$ km .

NB : The value of Δh_m is independent of the mass, charge or kinetic energy.

For Instance for an equatorial pitch angle of 11° the mirror point is closer to Earth: at $h_m = 1000$ km. when Dst = 0, and at $h_m = 1094$ km when Dst = -50nT.

This means that $\Delta h_m = 94$ km , provided of course that the initial radial distance is again at L = 3 in equatorial plane. (*see fig. 5)*

In the vicinity of the equatorial plane ($-40° < \lambda < +45°$) the altitudes (h_m) of all mirror points increase with time when Dst decreases: during main phases

$$\Delta h_{\mathbf{m}}(t) \sim -(1 / 3)\, R_E\, L^{\mathbf{3}}\, \Delta B_{eq} / B_E$$

$B(r) \sim r^{-3}$; $B_E = 31000$ nT ; $\Delta B_{eq} \mathbf{=} \Delta Dst < 0$

At low altitudes, L = 1 in the F2-region

$\Delta h_m = -(1/3) * 6671\text{ km} * (-50\text{ nT}) / 31000\text{ nT} = 3.4\text{ km}$

NB : Collisions do not inhibit the Betatron mechanism. They make the uplifting of h_m stepwise and discontinous, instead of uninterrupted and continous..

Fig ; 5

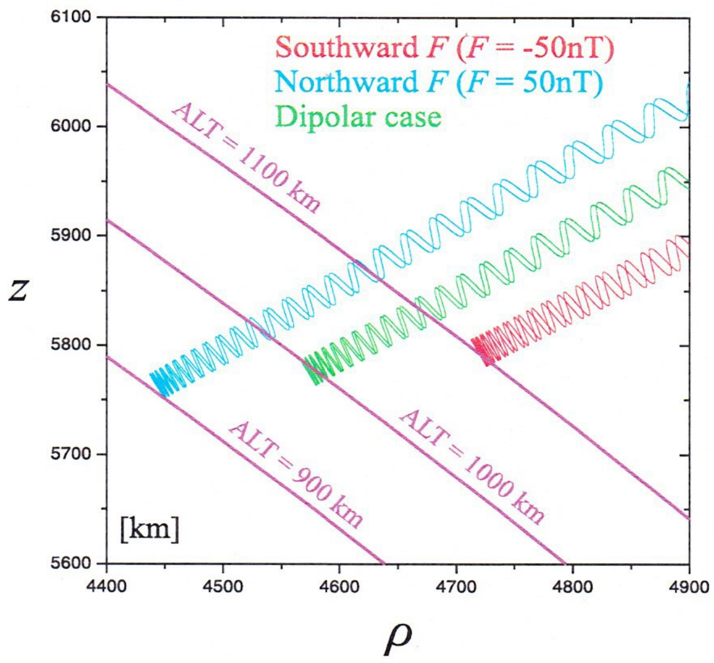

The mirror point altitude is the same for a 1 MeV proton and for a 10 eV electron, provided of course that they have the same initial equatorial pitch angle and the same initial equatorial distance.

Fig. 3. Meridian projections of the low altitude portions of the trajectories of a 10 MeV proton whose equatorial pitch angle is equal to 10.6° at $\rho_o = 3.0\ R_E$. The green trajectory is for a dipole magnetic field distribution. The blue one is for a dipole embedded in a northward IMF of +50 nT; the red one for a southward IMF ($F = -50$ nT).

Lemaire J.F, Batteux S.G. & Slypen I.N. (2005)
J. Atmosph.& Solar Terrestrial Physics, pp. 719;   doi: 10.1016/S0273-1177(03)00099-1)

Betatron mechanism has largest effects in the equatorial region,
where the magnetic field intensity is minimum along the trajectory of particles.

For a Dst-variation of $\Delta B_{eq} = \Delta Dst$ **=** -50 nT, ***Lemaire et al. (2005)*** verified that all mirror points altitudes are uplifted by $\Delta h_m = 94$ km along the drift shell L= 3.

This effect increases with equatorial distance of the drift shell (L).
For L = 6 and ΔDst **=** -50 nT, we verified that $\Delta h_m = 900$ km.

Lemaire J.F, Batteux S.G. & Slypen I.N. (2005)
J. Atmosph.& Solar Terrestrial Physics, pp. 719; doi: 10.1016/S0273-1177(03)00099-1)

NB : The Betatron mechanism should not be confused with types 1 & 2 Fermi mechanisms

.

Latitudes of Mirror Points

During a main phase the latitudes of all mirror points decrease; they shift closer to the equatorial plane as a result of the Betatron mechansim.
(shown in fig. 6)

The latitudinal shift of mirror points is largest at high altitudes, where it tends to compress most significantly the plasma toward the equatorial plane, and therefore to increase the omnidirectional flux in the equatorial region.

Fig. 6

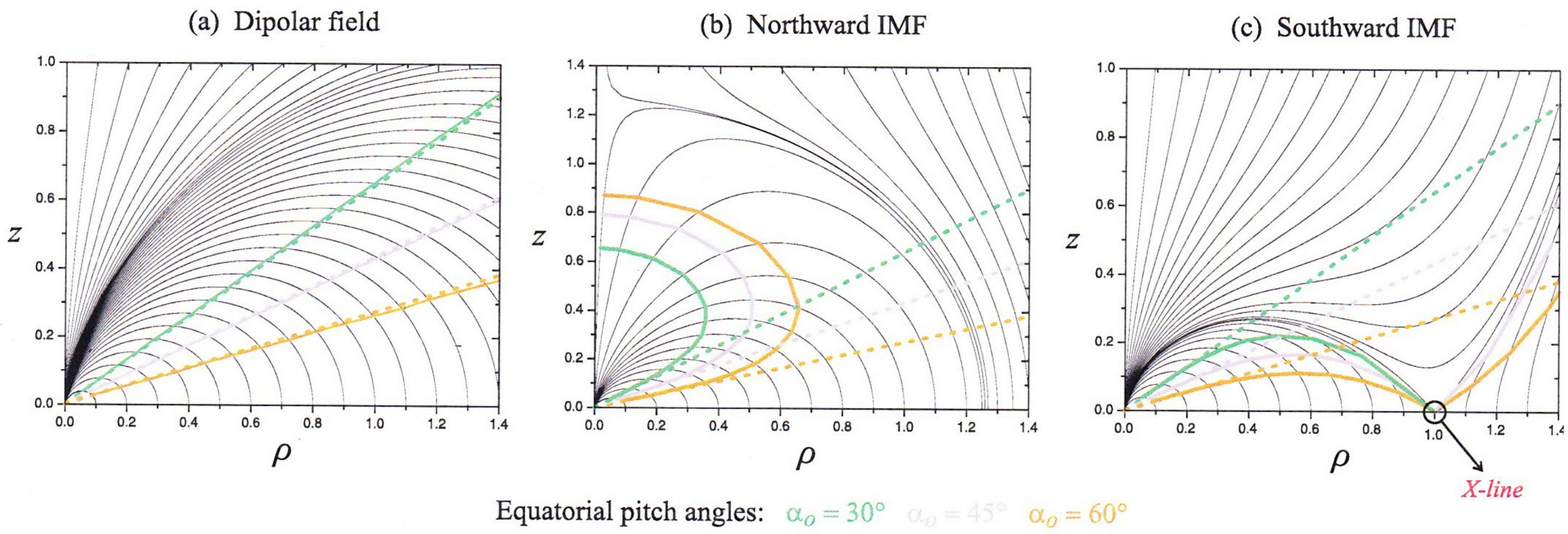

Fig. 2. Polar plots of magnetic field lines (black lines) and mirror points positions in three different magnetic field distributions: (a), dipolar case; (b), northward IMF; (c), southward IMF. On each figure, we have plotted the loci of the mirror points (straight coloured lines) and the dipolar Hamlin et al. (1961) approximate loci of mirror points (dashed coloured lines), for three values of the equatorial pitch angle ($\alpha_o = 30°$, $45°$ and $60°$). Compared to the dipolar case, we observe that mirror points latitude decreases and mirror points altitudes increase when $F < 0$ while, when $F > 0$, mirror points latitude increase, and mirror points altitude decrease. For a southward IMF, those conclusions are only valid below the *X-line* (see text).

Lemaire J.F, Batteux S.G. & Slypen I.N. (2005)
J. Atmosph.& Solar Terrestrial Physics, pp. 719; doi: 10.1016/S0273-1177(03)00099-1)

Betatron induced electric field

The induced electric field generated by the Betatron mechanism is determined by

$$\mathbf{E}(t) = E_\varphi \, \mathbf{e}_\varphi = - (\rho/2) \, (dB_z / dt) \, \mathbf{e}_\varphi$$

During a main phase $E_\varphi(t)$ is directed eastward (ρ is the distance from the oz axis in cylindrical coordinates)

NB : This eastward Betatron electric field might be related to, the *Prompt Penetration Field (PPF)* penetrating quickly down to equatorial latitudes .

Indeed, without giving it a well identified physical mechanism for the PPF, *Gonzales et al. (1979)* and *Fejer and Scherliess (1997)* felt that such a fast penetrating PPF should be induced in the ionosphere over a wide range of latitudes in order to account for ionospheric storms observations.

Time dependent integration of Lorentz equation of motion

Lemaire et al. (2005) **i**ntegrated numerically the equation of motion of charged particles for $B_z(t)$ and $E_\varphi(t)$ changing with time.

The linear variation of $B_z(t)$ and $E_\varphi(t)$ are illustrated in Panels a & b. of Fig. 5.

The altitudes and latitudes of the southern mirror points (h_m, λ_m),
the kinetic energy (W) of the decelerate/accelerated charged particle;
the magnetic field intensity at mirror point (B_m) ;
the magnetic field intensity in the equatorial plane (B_o),
are plotted in other panels of Fig. 5.
.

Fig. 5

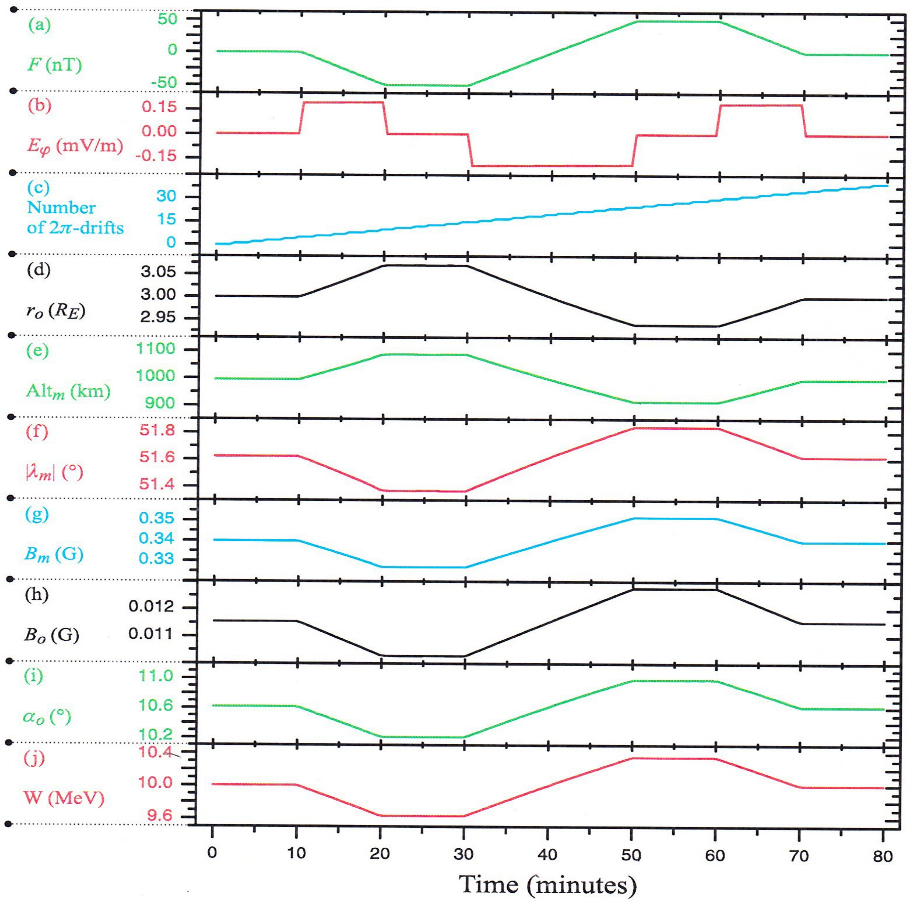

Fig. 5. Time variations of different parameters during a simulated drift of a proton of 10 MeV: (a) F in nT; (b) E_φ in mV/m; (c) number of complete drift around the Earth (around the dipole); (d) r_o in R_E; (e) altitude in km; (f) $|\lambda_m|$ in degree; (g) B_o in Gauss; (h) B_m in Gauss; (i) (relativistic) kinetic energy in MeV. Parameters (b), (d)-(i) refer to guiding centre positions computed from actual trajectory. For explanations, see text.

In *panel a* the linear change of the Dst-field variation is simulated.

The eastward induced electric field $E_\varphi(t)$ is shown in panel b.

The mirror point altitudes h_m (in km) are shown in panel h.

At the end of this run, F (or Dst) recovers its initial value.

The electric field, the kinetic energy, mirror point altitude and latitude ... recover all their initial values : the motion is adiabatic).

Lemaire J.F, Batteux S.G. & Slypen I.N. (2005)
J. Atmosph.& Solar Terrestrial Physics, pp. 719; doi: 10.1016/S0273-1177(03)00099-1)

Fig.6

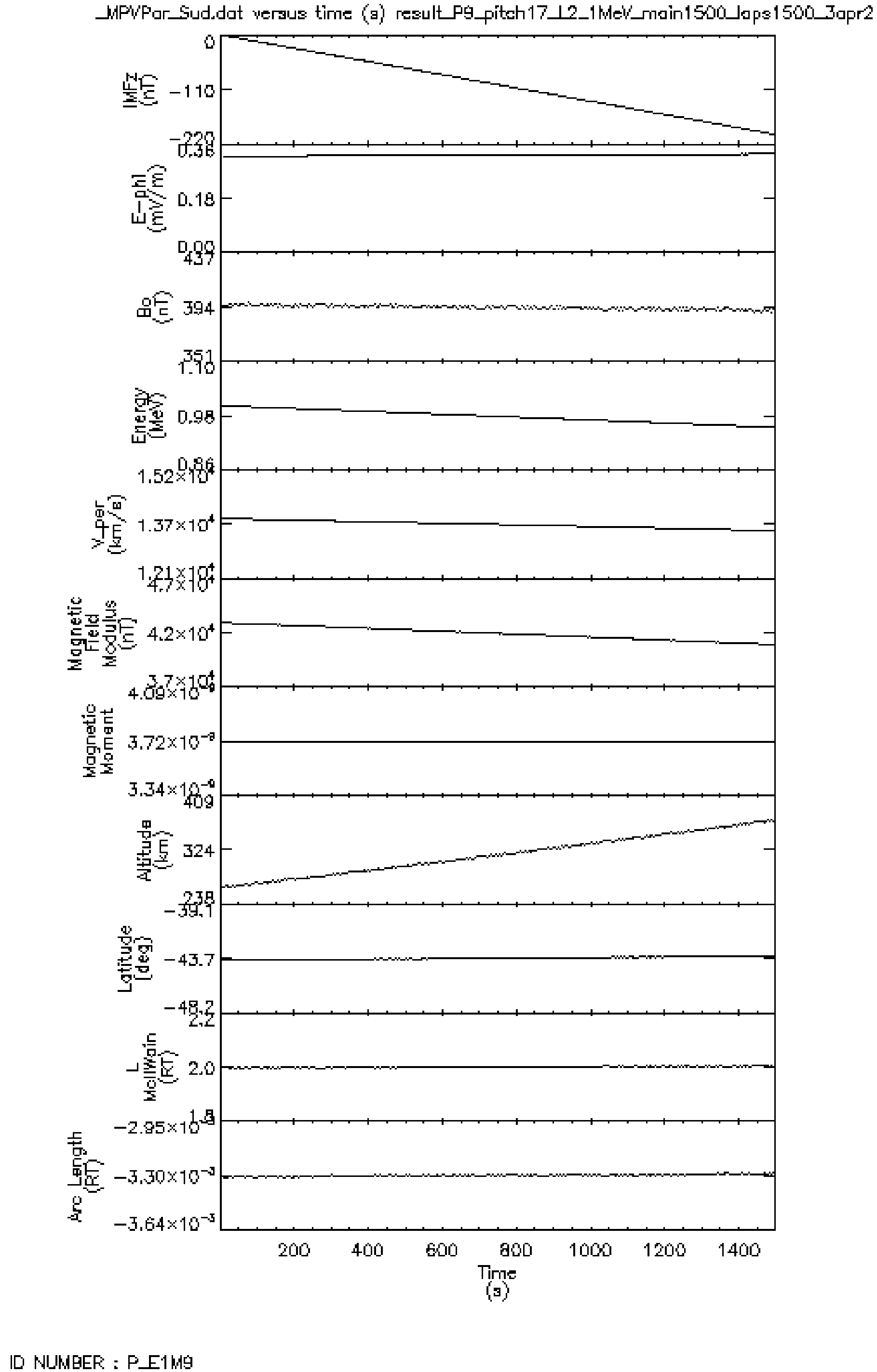

Similar plots for a « Main Phase like » linear decrease of the Dst-field variation (in panel a).

Eastward induced electric field $E_{\varphi}(t)$ (in panel b).

Mirror point altitude h_m (in km) (panel h).

Proton : 1 MeV
L= 2
Equatorial Pitch angle = 17°
Minimum Dst = -200 nT
Main Phase time = 1500 s
v_par mp = 0 km/s

Fig. 7

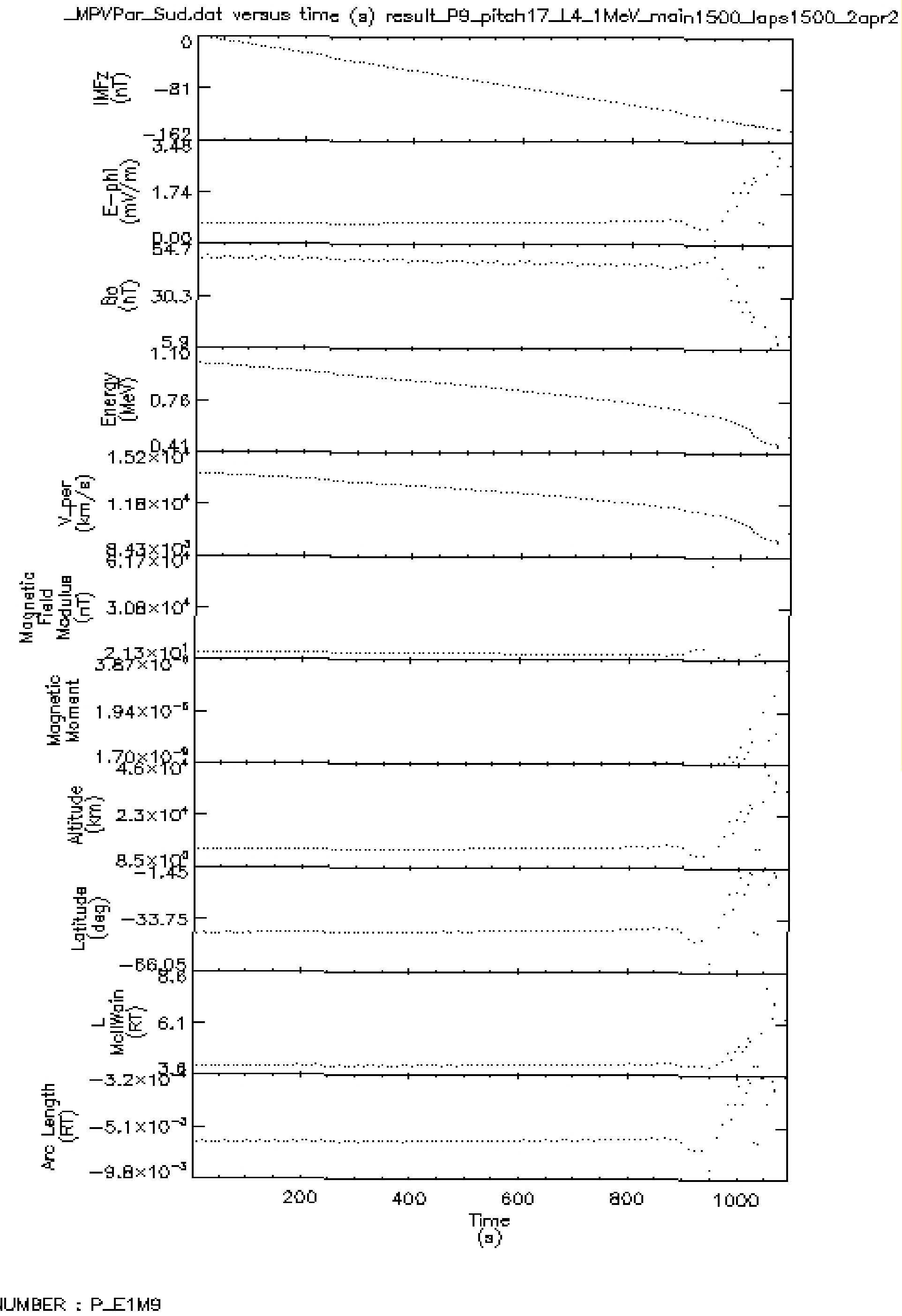

Similar plots for a « Main Phase like » linear decrease of the Dst-field variation (in panel a).

Eastward induced electric field $E_{\varphi}(t)$ (panel b).

Mirror point altitude h_m (in km) (panel h).

Note the violation of adiabatic behavior at the end of the trajectory. This occurs because the equatorial gyro-radius of this high energy particle is becoming too large...

Proton : 1 MeV
L= 4
Equatorial Pitch angle = 17°
Minimum Dst = -200 nT
Main Phase δt = 1500 s
v_par @ mp = 0 km/s

Fig. 8

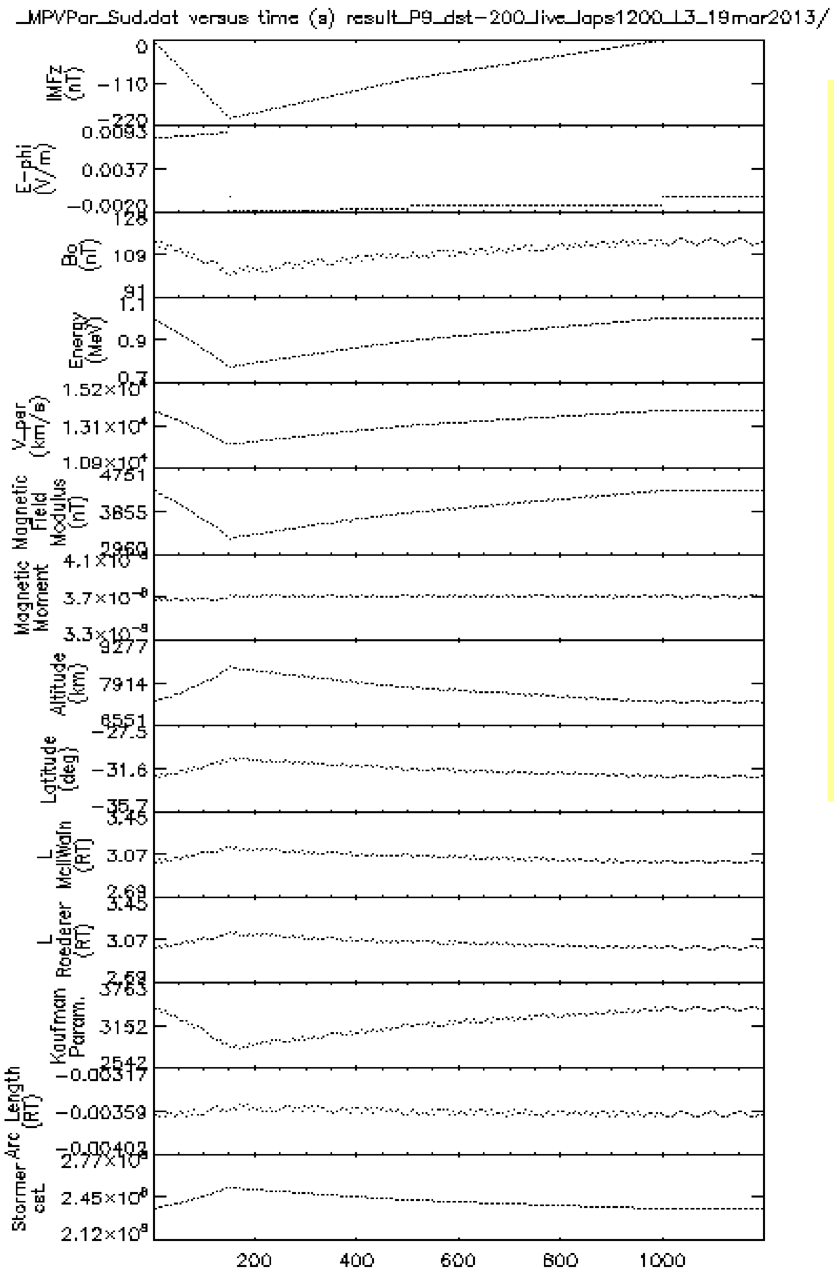

Similar plots for a ' main phase and recovery phase' of the Dst-field (in panel a).

Eastward induced electric field $E_{\varphi}(t)$ (in panel b)

Mirror point altitude h_m in km (in panel h)

A « reduced geomagnetic storm » model is used here.

Proton : 1 MeV
L= 3
Equatorial Pitch angle = 30°
Minimum Dst = -200 nT
Main Phase δt = 150 s
v_par @ mp = 0 km/s

ID NUMBER : P_E1M9

During main phases of geomagnetic storms guiding centers and mirror points are uplifted up to hundred km over equatorial latitudes.

This implies that in the equatorial region of the ionosphere and magnetosphere charged particles move higher up above the atmospheric layers, i.e. where they collide less frequently with neutrals and ions. Their trapping time is thus enlarged. As a matter of consequence, these particles accumulate then closer to the equatorial plane.

Furthermore, their loss cone angle shrinks faster than the equatorial pitch angle of the particles themselves. Due to this characteristic evolution the fluxes of trapped and precipitated particles at constant altitudes where measurements are made onboard of LEO satellites like SAMPEX, drop drastically during the main phase of geomagnetic storms. An alternative explaination for RB « drop outs » observed at low altitudes.

The droping of measured fluxes is very sharp/fast. Indeed, the vertical gradient of RB fluxes is very steep (positive upwards) at low altitudes. This implies that uplifting of mirror points by 100 km altitude (i.e. one atmospheric scale height) reduces the flux of trapped particles by orders of magnitudes over short periods of time after SSC.

Furthermore, as a consequence of the Betatron deceleration, the dramatic drop out of RB fluxes is emphasized by the decrease of the kinetic energy (W); indeed during main phases Betatron mechanism lowers the energy of the particles below the thresholds of particle detectors.

Uplifting of particles over equatorial latitudes and effects of pitch angle scattering

Since the equatorial loss cone angle becomes smaller when Dst decreases, almost no particles are precipitated in the atmosphere during main phases.

As a matter of consequence, the RB particles tend to pile up closer to the equatorial plane, as long as Dst continues descending. More and more particles accumulate high up, instead of decaying as during quiet pre-storm conditions.

Furthermore, due to non-resonant w-p scattering, the pitch angle distributions of the particles spreads along magnetic field lines: their mirror points diffuse away from the equatorial plane.

It is only at the end of main phases that the piling up in the upper equatorial region can eventually stop.

Therefore, at the begining of recovery phases the total amount of RB particles that have been stored above the atmosphere, will have significantly increased with respect to its pre-storm value. The total amount of particles accumulated depends on the total time duration the main phase did last.

The recovery phase ...

During recovery phases Dst increases. The reverse Betratron mechanism is then operating untill the end of the geomagnetic strom.

The mirror points return to lower altitudes closer to or into the atmosphere.
The equatorial loss cones angles become larger, and the fluxes of precipitated particles becomes larger again.

The rate of flux precipitation will even be boosted to higher values if the power spectrum of whislter waves is enhanced during the recovery phase.

Depending on the spectrum of waves interacting non-resonantly with RB electrons during the one or both phases of geomagnetic storms, as well as on the time length of the recovery phase and of the main phase, one expects the post-storm electron fluxes to be either larger, smaller or equal to their pre-storm values.

This is the main point we wished to make in this poster presentation at the EGU 2013.

Energization to relativistic energies

During recovery phases the electrons will be re-accelerated adiabatically by the Betatron mechanism. The most stably trapped electrons whose pitch angles are nearest to 90° (i.e. which are trapped in the equatorial region of the outer RB) may experience this non-adiabatic deceleration :acceleration cycle several times during consecutive geomagnetic storms.

How well this new scenario (without resonant w-p interactions) will be able to account for all observed non-adiabatic enhancements of RB fluxes, needs now to be worked out quantitatively, and should be tested by using existing measurements of relativistic electron fluxes both at high altitudes, close to the equatorial plane, as well as just above the atmosphere.

.

We hope this new scenario based on Betatron uplifting (and down-lifting) of RB particles during main phases (and recovery phases, respectively) will shade new light for understanding « drops outs » of trapped and precipitated fluxes that are observed during geomagnetic storms.

This new scenario is also expected to outline why during some geomagnetic storms post-storm trapped RB fluxes are either equal, smaller or larger than the pre-storm ones.

The end